Inversion of Abel's integral equation for experimental data

Moshe Deutsch and Israel Beniaminy

Citation: Journal of Applied Physics **54**, 137 (1983); doi: 10.1063/1.331739
View online: http://dx.doi.org/10.1063/1.331739
View Table of Contents: http://scitation.aip.org/content/aip/journal/jap/54/1?ver=pdfcov
Published by the AIP Publishing

Inversion of Abel's integral equation for experimental data

Moshe Deutsch and Israel Beniaminy
Department of Physics, Bar-Ilan University, Ramat-Gan, Israel

(Received 25 January 1982; accepted for publication 12 May 1982)

A stable high-accuracy method for calculating the inverse of Abel's integral equation for experimentally derived data is presented. The method employs a piece-wise cubic spline function, least-squares fitted to the data, to represent the function as inverted. Three formulas, two of which are based on the well-known analytic inverses of Abel's equation and a new one, which was recently developed by the authors and does not contain an explicit derivative, are given for calculating the inverse numerically. The results of numerical tests performed using these formulas on simulated data are presented and compared with the results obtained using other published methods. The comparative study indicates that our method, employing piece-wise least-squares cubic splines, accurately reproduces the inverse function, regardless of the inversion formula employed. It yields markedly better results than do all the other methods compared in this study, when highly error free, sparse, or very noisy data are inverted. The errors at the ends of the data interval ("termination errors") are also shown to be smaller than those of the other methods compared in this study.

PACS numbers: 52.70.Kz, 52.25.Ps, 06.50.Dc, 02.60.Nm

I. INTRODUCTION

Abel's integral equation is encountered in many research fields: shock wave tube and supersonic flow experimentation,[1] seismology,[2] study of electron emission from cathodes,[3] stereology,[4] radio astronomy,[5] atomic and molecular scattering,[6] and, most extensively, flame and plasma diagnostics.[7–9] In the last-mentioned field, Abel's equation describes the relation between the radial distribution function of the emission coefficient $g(r)$ of a cylindrically symmetric, optically thin extended radiation source, and the line-of-sight radiance $I(y)$ measured from outside the source. It is given by [7,9]:

$$I(y) = 2\int_y^1 g(r)r(r^2 - y^2)^{-1/2}\,dr, \tag{1}$$

where the radius of the source is normalized to unity. In practice, a set of discrete values of $I(y_i)$ $(i = 1,2,...n)$ are measured to a given accuracy and, since the physically relevant data is $g(r)$ rather than $I(y)$, one must invert Eq. (1) in order to obtain values of $g(r_i)$.

A large number of inversion methods were published over the years.[7–13] The overwhelming majority of these employ the explicit inversion formula, Eq. (2) below. However, since Abel's equation is by nature a slightly improperly posed problem,[12] any inversion method tends to amplify the random errors inherent in the measured $I(y_i)$ data. Thus, in order to obtain meaningful $g(r_i)$ values, measures must be taken to counteract this amplification as far as possible. In fact, the success of any inversion method is measured largely by its ability to cope with this problem. Through a number of detailed comparative studies,[7,12,13] the pseudoanalytic methods of Minerbo and Levy[13] (ML), the polynomial method of Cremers and Birkebak[7] (CB), and the spectral differentiation method of Anderssen,[11,12] established themselves as the best and most widely used methods. Since they were extensively discussed in the literature we shall not do so here. We would like, however, to point out a few features common to almost all published methods. First, the errors in the inverted $g(r_i)$ values near both ends of the data interval are invariably larger than those obtained at midinterval. This is the so-called termination error. Also, the accuracy of the inverted values diminishes rapidly as the number of available $I(y_i)$ data points decreases.[7] Consequently, in cases where very high-accuracy data is available almost all methods are unable to make full use of it in the sense that, even with closely spaced data, the mean standard deviation of the inverted $g(r_i)$ values from the accurate ones is much larger than the level of experimental errors in the $I(y_i)$ data.

We present here a new method, based on spline functions for inverting Abel's equation. By comparing the performance of our method for various examples to that of the best methods mentioned above, it is demonstrated that our method is much less plagued by the aforementioned diseases, while its accuracy exceeds that of the other method in difficult situations such as very high or very low levels of noise in the $I(y)$ data, or very sparse data. The method is presented in the next section. Numerical results obtained for a number of representative examples are given in the last section where a detailed discussion and comparison with other methods is also presented.

II. INVERSION METHOD

The well-known inversion formulas for Abel's integral equation, Eq. (1), are[14]

$$g^a(r) = -(1/\pi)\int_r^1 \frac{dI(y)}{dr}(y^2 - r^2)^{-1/2}\,dy, \tag{2}$$

and

$$g^b(r) = -(1/\pi)\frac{d}{dr}\left[\int_r^1 I(y)y(y^2 - r^2)^{-1/2}\,dy\right]. \tag{3}$$

Both of these require numerical differentiation of the experimentally derived $I(y_i)$ data, a process which greatly amplifies the experimental error inherent in the data. In view of this difficulty, a third, derivative-free inversion formula was

 0021-8979/83/010137-07$02.40

recently developed by the present authors[15]:

$$g^c(r) = -(1/\pi)\{[I(1)-I(r)](1-r^2)^{-1/2} + \int_r^1 [I(y)-I(r)]y(y^2-r^2)^{-3/2}\,dy\}. \quad (4)$$

The removable weak singularity of the integrand of all three inversion formulas at $y=r$ can, in general, be taken care of easily by one of the methods proposed by Davis and Rabinowitz.[16] In our spline-based method, however, this is not required since the singular terms cancel out.

Let us now represent $I(y)$ by a piece-wise cubic spline function[17]:

$$I(y) = \sum_{k=1}^{N-1} I_k(y), \quad (5)$$

where

$$I_k(y) = \begin{cases} 0, & y < \xi_k \\ a_k y^3 + b_k y^2 + c_k y + d_k, & \xi_k \leqslant y \leqslant \xi_{k+1} \\ 0, & \xi_{k+1} < y \end{cases}. \quad (6)$$

The quantities $\xi_1, \xi_2, \ldots \xi_N$ are the knots of the spline, and the cubic segments are so joined that both $I(y)$ and its first and second derivatives are continuous at the knots. It is also assumed that $I(y)$ vanishes for $y > \xi_N$.

Upon substitution of Eq. (5) in Eqs. (2)–(4) we obtain three corresponding inversion formulas in forms suitable for easy computer evaluation:

$$g^a(r) = -(1/\pi)\Big\{\sum_{k=i}^{N-1}[3a_k I_2(\xi_k,\xi_{k+1}) + 2b_k I_1(\xi_k,\xi_{k+1}) + c_k I_0(\xi_k,\xi_{k+1})] + 3a_{i-1}I_2(r,\xi_i) + 2b_{i-1}I_1(r,\xi_i) + c_{i-1}I_0(r,\xi_i)\}, \quad (7)$$

$$g^b(r) = -(1/\pi r)\Big\{\sum_{k=i}^{N-1}[a_k J_4(\xi_k,\xi_{k+1}) + b_k J_3(\xi_k,\xi_{k+1}) + c_k J_2(\xi_k,\xi_{k+1}) + d_k J_1(\xi_k,\xi_{k+1})] + a_{i-1}J_4(\xi_i) + b_{i-1}J_3(\xi_i) + c_{i-1}J_2(\xi_i) + d_{i-1}J_1(\xi_i)\} + (1/\pi) \times [a_{i-1}(3r^3\ln r/2 + 3r^3/8) + c_{i-1}(r\ln r + r/2)], \quad (8)$$

$$g^c(r) = -(1/\pi)\Big\{\sum_{k=i}^{N-1}[a_k K_4(\xi_k,\xi_{k+1}) + b_k K_3(\xi_k,\xi_{k+1}) + c_k K_2(\xi_k,\xi_{k+1}) + d_k K_1(\xi_k,\xi_{k+1})] + a_{i-1}K_4(\xi_i) + b_{i-1}K_3(\xi_i) + c_{i-1}K_2(\xi_i) + d_{i-1}K_1(\xi_i)\} + (1/\pi)[3a_{i-1}r^2\ln r/2 + c_{i-1}\ln r], \quad (9)$$

where i is the index of the smallest knot larger than the argument r for which $g(r)$ is currently being calculated, and

$$I_n(a,b) \equiv I_n(a) - I_n(b) = \int_a^b y^n(y^2-r^2)^{-1/2}\,dy,$$

$$J_n(a,b) \equiv J_n(a) - J_n(b), = \frac{d}{dr}[I_n(a) - I_n(b)] = \frac{d}{dr}[I_n(a,b)], \quad (10)$$

$$K_n(a,b) \equiv K_n(a) - K_n(b) = \int_a^b y^n(y^2-r^2)^{-3/2}\,dy.$$

Analytic values of these functions are listed in Table I. Note that none of the functions is singular even at $r=1$, since once we assumed an explicit functional form for $I(y)$ the singular terms canceled out as mentioned earlier.

The reasons for choosing a spline-function representation for $I(y)$ are the following. Both the function and its first derivative are continuous and smooth, so that its use in Eqs. (2)–(4) is not liable to cause numerically undesirable effects. Also, the spline function is known to have excellent smoothing properties.[18] Thus, both oversmoothing of important structure latent in the data and amplification of spurious oscillations are eliminated. Finally, due to the piece-wise nature of the function, random errors or "bad" values in one section of $I(y)$ will not influence the quality of the fit in other sections of $I(y)$. In particular, the larger fitting errors invariably encountered near the ends of the data interval,[12] especially when $I(y)$ is still appreciably large at the endpoints, will be confined to the end sections of the spline functions. Since the relative weight of these end sections in the sums of Eqs. (7)–(9) is larger the closer r is to the endpoints, it is expected that the piece-wise nature of the spline will confine these so-called termination errors to the end sections of the inverted $g(r)$ function. This is indeed borne out by the examples presented below. By contrast, Anderssen[12] found this particular type of error to introduce large errors in the inverted $g(r)$ values over a wide argument internal in almost all of the existing inversion methods.

III. DISCUSSION OF NUMERICAL RESULTS

A. Test examples

From the numerous examples investigated by us, we have chosen four pairs of $g(r)$–$I(y)$ functions for a detailed discussion in this section. These are listed in Table II and presented graphically in Fig. 1. They were widely used in previously published comparative studies[7,12,13] of Abel inversion methods so that our results can readily be compared with those obtained from a large number of other methods.

TABLE I. Values of the integrals in Eq. (10). Note: $u \equiv (y^2-r^2)^{1/2}$.

n	$I_n(y)$	$J_n(y)$	$K_n(y)$
0	$\ln(y+u)$	$-r/(yu+u^2)$	
1	u	$-r/u$	$-1/u$
2	$yu/2 + r^2\ln(y+u)/2$	$-ry/(2u) + r^2\ln(y+u) - r^3/(2yu+2u^2)$	$-y/u + \ln(y+u)$
3	$u^3/3 + r^2u$	$-ur + 2ru - r^3u$	$u - r^2u$
4	$y^3u/4 + 3r^2yu/8 + 3r^4\ln(y+u)/8$	$-y^3r/(4u) + 3ryu/4 - 3r^3y/(8u) + 3r^2\ln(y+u)/4 - 3r^5/(8yu+8u^2)$	$yu/2 - r^2y/u + 3r^2\ln(y+u)/2$

TABLE II. Test function pairs used in the numerical tests. For details see text. Note: $u=(1-y^2)^{1/2}$, $v=(1/4-y^2)^{1/2}$, $w=(1/16-y^2)^{1/2}$.

n	$g_n(r)$		$I_n(y)$	
1	$1-3r^2+2r^3$	$0<r<1$	$u\left(1-\frac{5}{2}y^2\right)+\frac{3}{4}y^4\ln\frac{1+u}{y}$	$0<y<1$
2	$1-2r^2$	$0<r<\frac{1}{2}$	$\frac{4}{3}(1+2y^2)u-\frac{2}{3}(1+8y^2)v-4y^2\ln\frac{1+u}{\frac{1}{2}+v}$	$0<y<\frac{1}{2}$
	$2(1-r)^2$	$\frac{1}{2}<r<1$	$\frac{4}{3}(1+2y^2)u-4y^2\ln\frac{1+u}{y}$	$\frac{1}{2}<y<1$
3	$\frac{3}{4}+12r^2-32r^3$	$0<r<\frac{1}{4}$	$\frac{32}{27}u(1-7y^2)+\left(\frac{1}{108}+\frac{566}{27}y^2\right)w+\frac{96}{27}y^2(1+y^2)\ln\frac{1+u}{\frac{1}{4}+w}-24y^2\ln\frac{\frac{1}{4}+w}{y}$	$0<y<\frac{1}{4}$
	$\frac{16}{27}(1+6r-15r^2+8r^3)$	$\frac{1}{4}<r<1$	$\frac{32}{27}u(1-7y^2)+\frac{96}{27}y^2(1+y^2)\ln\frac{1+u}{y}$	$\frac{1}{4}<y<1$
4	$10+16(\frac{1}{2}-r)^2\sin(8\pi r-\frac{1}{2}\pi)$	$0<r<\frac{1}{2}$	$\int_y^1\frac{g_4(r)r}{(r^2-y^2)^{1/2}}dr$ use numerical integration	$0<y<\frac{1}{2}$
	$10+100(\frac{1}{2}-r)^2$	$\frac{1}{2}<r<1$	$\frac{10}{3}(11+40y^2)-100y^2\ln\frac{1+u}{y}$	$\frac{1}{2}<y<1$

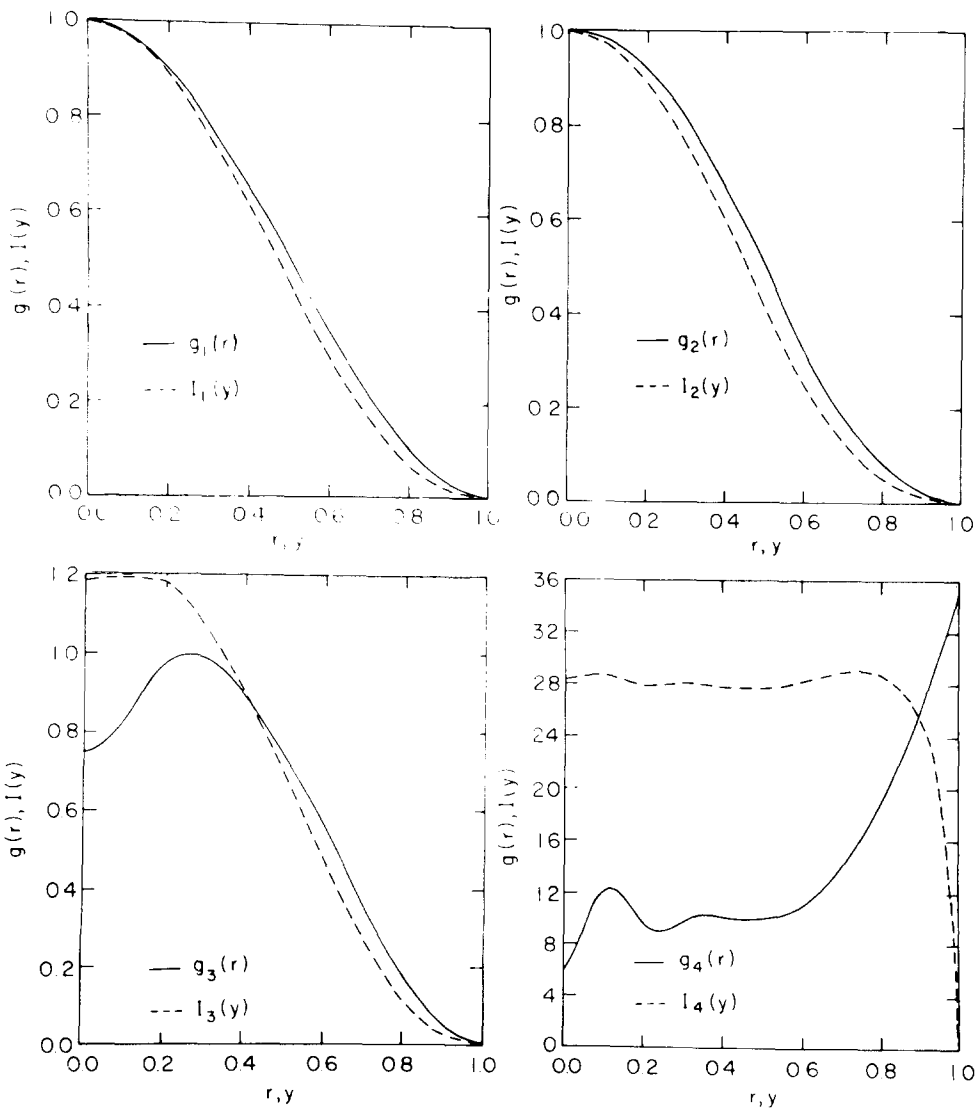

FIG. 1. Graphical presentation of the four test function pairs of Table II.

The tests were aimed at assessing the behavior of our method for varying levels of random "experimental" error and/or varying density of data points in the measurement interval.

The first three pairs of functions in Table II closely resemble radiance-emission coefficient functions obtained in plasma diagnostics.[7] As Cremers and Birkebak[7] pointed out, the off-axis peaked $g_3(r)$ function is much more difficult to reproduce faithfully than the two bell-shaped functions $g_1(r)$ and $g_2(r)$. The last pair of functions closely resembles supersonic flow[1] and shock wave tube[11,12] data. $I_4(y)$ differs from I_1-I_3 by its near discontinuity at $y = 1$, and $g_4(r)$ also differs from g_1-g_3 by increasing, rather than decreasing as $r \rightarrow 1$. This function was found to be a stumbling block for all Abel inversion mehtods except that of Anderssen.[12]

B. Computer programs

Two FORTRAN programs were developed. The first of these generates $I(y_i)$ values for a given $g(r)$ function. The number of equally spaced data points as well as the amplitude of the normally distributed random error to be added to the simulated $I(y_i)$ data are user defined.

The second program (available from the authors) is an implementation of the method presented in the previous section. For a given set of $I(y_i)$ data, the user may choose either g^a, g^b or g^c [Eqs. (7)–(9)] to calculate the corresponding values of $g(r)$. The program also calculates the absolute error at each point

$$G^{a,b,c}(r_i) = |g^{a,b,c}(r_i) - g(r_i)|,$$

wherever exact values of the inverted function $g(r)$ are available, and also the mean standard deviation $\sigma(n, m)$ defined by[12]:

$$\sigma(n, m) = \left[\left\{ \sum_{i=n}^{m} [g^{a,b,c}(r_i) - g(r_i)]^2 \right\} / (m - n + 1) \right]^{1/2},$$

where $g^{a,b,c}$ denotes g^a, g^b or g^c as requested by the user.

C. Comparative study of results

Results obained with our method for the first three examples, using a varying number of data points in the measurement interval, are given in Table III. S denotes the mean standard deviation of the input $I(y_i)$ data from the exact values. The mean standard deviations, $\sigma(1, n)$, in $g(r)$ listed in the table were obtained for error-free, 14-digit precision data, as well as $I(y_i)$ data rounded off to two decimal digits to simulate experimental errors.[7,12,13] This rounding procedure is equivalent[13] to the inclusion in $I(y_i)$ normally distributed random noise with a mean standard deviation of $S = 0.00289$. The table also lists results obtained for the same functions by different authors under identical conditions.

Two trends clearly emerge from our results. First, for error-free data, although σ is already very small for even sparse data (10 points), the accuracy rapidly increases upon increasing the number n of data points in the interval. This is best demonstrated by the results obtained for I_1 with $S = 0$. In the other methods the rate of decrease in σ on increasing n is much smaller and there are indications that at about $n = 50$ σ bottoms for these methods at a value higher than ours. Thus, when high accuracy and closely spaced data are

TABLE III. Mean standard deviations $\sigma(1,n)$ obtained for the first three function pairs of Table II. g^a and g^c denote results obtained with our method Eqs. (7) and (9) in text. F is Frie's method Ref. 19, and CB 4 is Cremers and Birkebak's fourth degree polynomial method, Ref. 7. Data for F and CB4 were taken from Ref. 7. Values in this and the following tables are presented in the form $a \times 10^b$.

		$S = 0$								$S = 2.89 \times 10^{-3}$					
		F		CB4		g^a		g^c		F		CB4		g^c	
I_n	n	a	b	a	b	a	b	a	b	a	b	a	b	a	b
I_1	10	2.4	−3	1.8	−1	1.3	−3	1.3	−3	8.4	−2	1.8	−1	1.5	−2
	20	6.5	−4	4.0	−4	6.8	−4	6.8	−4	1.3	−2	6.7	−3	4.5	−3
	30	3.0	−4	1.3	−4	1.9	−4	1.9	−4	2.1	−2	3.7	−3	2.8	−3
	40	1.7	−4	7.8	−5	4.3	−5	4.2	−5	2.5	−2	6.0	−3	4.1	−3
	50	1.1	−4	6.5	−5	4.3	−5	4.3	−5	2.5	−2	5.7	−3	3.4	−3
	100					2.7	−6	2.5	−6					3.2	−3
	200					1.2	−6	3.3	−7					3.3	−3
I_2	10	3.1	−3	1.8	−1	2.5	−2	2.5	−2	8.0	−3	1.8	−1	2.4	−2
	20	7.9	−4	1.5	−3	9.5	−4	9.5	−4	1.4	−2	4.2	−3	5.0	−3
	30	3.5	−4	9.2	−4	2.9	−4	2.9	−4	1.7	−2	7.1	−3	7.0	−3
	40	2.0	−4	7.6	−4	1.6	−4	1.6	−4	2.3	−2	7.0	−3	5.3	−3
	50	1.3	−4	7.0	−4	1.5	−4	1.5	−4	2.3	−2	5.3	−3	3.2	−3
	100	5.6[a]	−3	3.2[b]	−3	2.7	−5	2.7	−5	4.0[a]	−3	4.5[b]	−3	5.7	−3
	200					4.8	−6	4.8	−6						
I_3	10	6.4	−3	2.1	−1	1.2	−1	1.2	−1	1.6	−2	2.1	−1	1.2	−1
	20	1.7	−3	3.5	−3	3.5	−3	3.5	−3	1.5	−2	1.0	−2	4.2	−3
	30	7.5	−4	1.8	−3	2.4	−3	2.4	−3	2.2	−2	1.0	−2	5.2	−3
	40	4.3	−4	1.3	−3	4.1	−4	4.1	−4	2.3	−2	9.9	−3	5.0	−3
	50	2.8	−4	1.1	−3	3.8	−4	3.8	−4	1.9	−2	1.1	−2	5.6	−3
	100					5.4	−5	5.5	−5						
	200					8.8	−6	8.8	−6						

[a] Results obtained by AII method.
[b] Results obtained by ML 7 method.

TABLE IV. Deviations $G(r_i)$ of the inverted results from the accurate ones obtained with equally spaced, error-free data using $I_2(y_i)$ $(i = 1,2,...101)$. AI and AII denote Anderssen's methods, Ref. 12, ML7 denotes Minerbo and Levy's seventh degree polynomial method, Ref. 13, and $g^a(r)$ is our method, Eq. (7).

	$G(r_i)$							
	AI		AII		ML7		g^a	
r	a	b	a	b	a	b	a	b
0.01	3.2	−2	5.6	−2	3.1	−3	1.4	−7
0.1	1.2	−4	1.7	−4	1.0	−3	5.5	−7
0.2	1.6	−5	1.4	−4	2.7	−3	2.1	−7
0.3	1.1	−5	1.3	−4	3.2	−3	4.0	−7
0.4	9.5	−6	1.3	−4	1.1	−3	6.7	−7
0.5	1.6	−3	9.2	−5	1.9	−3	5.0	−5
0.6	1.0	−5	3.1	−5	3.1	−3	1.9	−6
0.7	6.1	−6	7.8	−6	4.7	−4	8.5	−7
0.8	8.6	−6	9.2	−6	3.8	−3	5.0	−6
0.9	7.9	−5	2.2	−5	1.1	−3	2.5	−5
1.0	1.3	−1	1.4	−5	9.6	−3	8.3	−3

available, our method is able to make full use of it while F and CB are not.

The other trend relates to the behavior of the different methods as the random error in $I(y_i)$ increases. Compare the results listed in Table III for the F and CB methods with and without noise. The stability of the pseudoanalytic CB method against noise is much better than that of the F method. The superiority of the pseudoanalytic methods over other methods in this respect was already commented on by Minerbo and Levy[13] and Anderssen.[11,12] Note, however, that for sparse data, our method outperforms even the CB method by almost an order of magnitude for I_1 and I_2, and a factor of 2–3 for I_3. Moreover, as the number of points increases, our method very rapidly attains a σ level close to that of the input data. For $S = 2.89\times10^{-3}$ we obtain $\sigma = 4.2\times10^{-3}$–$5\times10^{-3}$ for only 20 data points in all three examples! While the σ level attained by the CB4 method is only slightly higher for I_1 and I_2, for I_3 the σ value of CB is twice as high as ours. This trend continues and even increases in magnitude for higher levels of error in the $I(y_i)$ data.

Note that although the derivative-free inversion formula $g^c(r)$ yields slightly better results where the full accuracy of the $I(y_i)$ data is realizable, i.e., error-free data, easy-to-invert function, and a large number of data points, in all other cases, and in particular when even a small level of random error is present in the $I(y)$ data, all three inversion formulas [Eqs. (7)–(9)] yield practically identical results. This is due to the excellent smoothing properties of the least-squares fitted spline function which prevent error amplification. Since g^a, g^b, and g^c yield the same results we have listed only those obtained for g^c, except for the $S = 0$ data.

Finally, note that the methods of Anderssen[11,12] and Minerbo and Levy,[13] for which data were published for I_2 and $n = 100$ only, fail for error-free data and yield values of σ an order of magnitude larger than that of CB and F, and 2 orders of magnitude larger than our method! This is rather surprising in view of their excellent behavior for noisy data. In the case of Anderssen's method this is largely due to its inability to copy successfully with termination errors near $r = 0$, as can be seen from Table IV, which lists results ob-

TABLE V. Mean standard deviations obtained for I_2 and $n = 100$ with different levels of input error. Notation is identical with that of Table IV.

	AI		AII		ML7		g^a	
	a	b	a	b	a	b	a	b
$S = 0$								
$\sigma(1,101)$	8.9	−4	5.6	−3	3.2	−3	2.7	−5
$\sigma(6,96)$	3.2	−4	1.1	−4	2.6	−3	2.8	−5
$\sigma(11,91)$	2.8	−4	9.8	−5	2.6	−3	2.9	−5
$S = 0.002\,89$								
$\sigma(1,101)$	9.8	−3	4.0	−3	4.5	−3	6.1	−3
$\sigma(6,96)$	2.9	−3	2.7	−3	4.0	−3	3.9	−3
$\sigma(11,91)$	2.4	−3	2.8	−3	3.9	−3	2.6	−3
$S = 0.01$								
$\sigma(1,101)$	1.6	−2	7.6	−3	9.0	−3	1.8	−3
$\sigma(6,96)$	7.0	−3	6.1	−3	8.7	−3	1.8	−3
$\sigma(11,91)$	6.4	−3	5.8	−3	8.3	−3	1.9	−3
$S = 0.1$								
$\sigma(1,101)$	6.6	−2	5.6	−2	7.2	−2	1.5	−2
$\sigma(6,96)$	6.6	−2	5.4	−2	7.3	−2	1.4	−2
$\sigma(11,91)$	6.3	−2	5.5	−2	7.0	−2	1.3	−2

TABLE VI. Deviations obtained for 100 equally spaced error-free $I_4(y)$ data points. PV7 denotes the seventh degree Chebyshev polynomial method of Piessens and Verbaeten, Ref. 20. Other notations are identical with those of Table IV.

	$G(r_i)$							
	ML7		PV7		AII		g^c	
r	a	b	a	b	a	b	a	b
0.01	−4.3	0	−4.7	0	3.9	0	1.4	−2
0.05	−1.5	0	−2.5	0	2.3	−2	−5.8	−4
0.1	1.6	0	1.2	0	1.6	−2	−7.0	−3
0.15	1.2	0	1.5	0	1.8	−1	3.7	−3
0.20	−7.0	−1	−3.4	−1	−6.4	−3	−3.2	−3
0.25	−1.1	0	−1.1	0	−1.0	−2	−4.2	−3
0.30	1.9	−1	−3.2	−1	1.2	−3	−9.2	−4
0.35	4.2	−1	4.1	−1	4.7	−3	−3.1	−3
0.40	3.2	−1	3.7	−1	−1.4	−4	3.9	−3
0.45	1.4	−1	1.4	−1	−1.2	−3	−2.9	−3
0.50	−2.8	−2	−2.0	−2	−1.3	−3	−1.2	−3
0.55	−1.9	−1	−2.0	−1	−3.9	−3	−3.2	−3
0.60	−1.6	−1	−1.6	−1	−4.7	−3	−5.1	−3
0.65	−4.7	−2	−1.5	−2	−5.4	−3	−5.1	−3
0.70	6.1	−2	1.1	−1	−5.9	−3	−1.0	−2
0.75	9.2	−2	1.1	−1	−6.3	−3	1.1	−3
0.80	2.3	−2	6.7	−3	−6.7	−3	2.9	−2
0.85	−9.0	−2	−1.1	−1	−7.2	−3	1.6	−1
0.90	−1.1	−1	−6.5	−2	−8.0	−3	−5.5	−3
0.95	9.6	−2	1.4	−1	1.9	−3	2.2	−1
1.0	−1.9	0	−2.1	−1	3.2	−1	1.5	0

tained with different methods for I_2. Note the exceptionally small and constant level of error in the $g^a(r_i)$ values over practically all of the data interval. This indicates that for $n \approx 100$ our inversion method is very accurate and so the inversion as such should add only an extremely small amount of noise to that inherent in the $I(y_i)$ data. We have therefore tested our method extensively with I_2 and $n = 100$ for a varying level of random noise in the $I(y_i)$ data. The results, together with those obtained by Anderssen[12] under identical conditions are summarized in Table V.

First note that the errors obtained using our method are lower than those obtained with either the A or ML methods by a factor ranging from 3–4 (for $S = 0.1$) to 2 orders of magnitude (for $S = 0$). The table also shows that for S levels larger than $\sim 10^{-3}$ in the input data, the error level in the $g^a(r_i)$ values is actually lower than that of the input. This is due to the effective smoothing accomplished by least-squares fitting of the spline function to the $I(y_i)$ data.[18] Furthermore, note that with our method $\sigma(1,101) \approx \sigma(6,96) \approx \sigma(11,91)$ for practically all S levels of the input $I(y_i)$ data. This indicates that no appreciable termination errors occur in the $g^a(r_i)$ values. This behavior was anticipated in view of the piece-wise nature of the spline function as discussed earlier. By contrast, large termination errors are discernible in the other methods listed in Table V. The stability of our method to localized small perturbations was also checked using the method suggested by Minerbo and Levy.[13] Both global stability, i.e., stability of the value of $\sigma(1,101)$ and local stability, were found to be the same as those of method II of Anderssen.[12]

Finally, Table VI presents results obtained for I_4 of Table II. As the results listed in the first two columns demonstrate, even the best pseudoanalytic methods fail to stabilize for such data. This was first pointed out by Anderssen,[11,12] whose spectral differentiation based method[12] yields results on the same level of accuracy as ours over most of the data interval. On the upper fifth of the interval, $0.8 \leqslant r \leqslant 1$, however, the AII method is clearly superior to ours, while our method clearly outperforms AII on the lower fifth, $0 \leqslant r \leqslant 0.2$ of the interval.

On the basis of the large body of numerical tests performed by us, out of which only a small, although typical, portion was presented here, we may safely conclude that our spline-based inversion method is highly accurate, stable against both small localized perturbations and overall experimental noise, and has much lower termination errors than all of the other methods it was compared with. It yields markedly better results than do those methods when highly error-free, very sparse, and/or very noisy data are inverted.

[1] R. W. Ladenberg and D. Bershader, *Physical Measurements in Gas Dynamics and Combustion in High Speed Aerodynamics and Jet Propulsion*, Vol. 9 (Oxford University, Oxford, 1957).
[2] K. E. Bullen, Geophys. J. R. Astron. Soc. **4**, 93 (1961).
[3] E. L. Kosarev, Comput. Phys. Commun. **20**, 69 (1980).
[4] A. J. Jakeman and R. S. Anderssen J. Microscopy Oxford **105**, 121 (1975).
[5] R. N. Bracewell, Austral. J. Phys. **9**, 198 (1956).
[6] U. Buck, Rev. Mod. Phys. **46**, 369 (1974).
[7] C. J. Cremers and R. C. Birkebak, Appl. Opt. **5**, 1057 (1966).
[8] R. Illingworth, R. K. Thareja, A. Raven, P. T. Rumsby, J. A. Stamper, and O. Willi, J. Appl. Phys. **51**, 1435 (1980); A. Kuthy, Nucl. Instrum. Methods **180**, 17 (1981).
[9] W. L. Barr, J. Opt. Soc. Am. **52**, 885 (1962).
[10] A. Kuthy, Nucl. Instrum. Methods **180**, 7 (1981); S. J. Young, J. Quant. Spectrosc. Radiat. Transfer **25**, 479 (1981); R. O. Sirola and T. P. Anderson, Rev. Sci. Instrum. **38**, (1967); R. Illingworth and R. K. Thareja, J. Phys. E **14**, 147 (1981).
[11] R. S. Anderssen, in *Error, Approximation and Accuracy*, edited by F. R. de Hoog and C. L. Jarvis (University of Queensland, Brisbane, 1973), p. 61.
[12] R. S. Anderssen, J. Inst. Math. Its Appl. **17**, 329 (1976).

[13]G. N. Minerbo and M. E. Levy, Society for Industrial and Applied Mathematics J. Numer. Anal. **6**, 598 (1969).
[14]E. T. Whittaker and G. N. Watson, *A Course of Modern Analysis* (Macmillan, New York, 1948).
[15]M. Deutsch and I. Beniaminy, Appl. Phys. Lett. **41**, 27 (1982).
[16]P. S. Davis and P. Rabinowitz, *Methods of Numerical Integration* (Academic, New York, 1975), Sec. 2.12.
[17]J. H. Ahlberg, E. N. Nielson, and J. L. Walsh, *The Theory of Splines and Their Application* (Academic, New York, 1967).
[18]M. J. D. Powell, Rep. No. HL67/5309 (AERE Harwell, Didcot, Oxon OX11 ORA, England, 1967).
[19]W. Frie, Ann. Phys. NY **10**, 332 (1963).
[20]R. Piessens and P. Verbaeten,Nordisk Tidsskrift for Informationsbehandling **13**, 451 (1973).